RSC Advances

ROYAL SOCIETY OF CHEMISTRY

www.rsc.org/advances

RSC Advances

COMMUNICATION

Protonation and axial ligation intervened fluorescent turn-off sensing of picric acid in freebase and tin(IV) porphyrins

Received 00th January 20xx,
Accepted 00th January 20xx

DOI: 10.1039/x0xx00000x

www.rsc.org/

Rahul Soman, Subramaniam Sujatha and Chellaiah Arunkumar*

Freebase and tin(IV)-porphyrins are examined for the selective detection of picric acid and the affinity is revealed by spectroscopic titrations and X-ray structures. The sensing is mediated through protonation and axial ligation succeeded in 1-5 and 6-9 respectively. Fluorescent lifetime studies show that the quenching is dynamic in freebase and static in tin(IV)-porphyrins.

In recent years, trace detection of powerful explosive nitroaromatic compounds (NACs) is an active area of research owing to their increasing concern over environmental and homeland security.[1] In particular, picric acid (PA) is a strong organic acid, extremely hazardous and widely found in explosives.[2] Among the various analytical methods employed so far to track down NACs, fluorescence based sensing techniques are the most effective tool due to their high sensitivity, specificity and fast response times.[3] A number of fluorescent materials have been identified based on macrocycles such as anthryl calix[4]arene,[4] and porphyrins/phthalocyanines,[5] small organic molecules,[6] conjugated polymers,[7] green materials,[8] Schiff base complexes[9] and metal–organic frameworks[10] that show a selective response towards PA. Porphyrin based fluorescent sensors[11] are extensively studied because of their ease of synthesis, excellent sensitivity and characteristic photophysical properties like pronounced photostability, high fluorescence quantum yield, tunable fluorescence emission etc. The highly conjugated freebase porphyrin core is able to accommodate various metal ions due to its strong coordination ability and hence it also acts as the metal ion sensors. Here, we describe a series of freebase and high valent tin(IV) *meso*-tetraarylporphyrins (Scheme 1), which exhibit highly selective responses towards PA comparing to other NACs, where hydrogen bonding, protonation and axial ligation are the key factors for their sensitivity and selectivity.

The freebase and tin(IV) derivatives are synthesized using literature methods[12,13] and characterized by UV-Visible, ^{1}H NMR and single crystal X-ray analysis. The photophysical data of porphyrins **1**–**9** are given in Table S1. The optical absorption spectra of freebase porphyrins exhibit an intense Soret band between 419-423 nm and four weaker visible (Q) bands whereas tin(IV) porphyrins show strong Soret absorption between 426-432 nm with two characteristic weaker Q bands.[14] On excitation at the Soret band, porphyrins **1**–**9** exhibit two well-defined emission bands between 603-722 nm ($S_1 \rightarrow S_0$) and a weak emission between 433-467 nm ($S_2 \rightarrow S_0$).[15]

To observe the sensing ability of porphyrins, **1**–**9** against various NACs, fluorescence titration experiments were performed with porphyrins in $CHCl_3$ (1 x 10^{-8} M) by the addition of micromolar solutions of various analytes (in $CHCl_3$) such as nitrobenzene (NB), phenol, 2-nitrophenol (2-NP), 4-nitrophenol (4-NP), 2,4-dinitrophenol (2,4-DNP), 2,4,6-trinitrophenol (PA), 2,4,6-trinitrotoluene (TNT), acetic acid (AA) and 2,3-dichloro-5,6-dicyano-1,4-benzoquinone (DDQ). Notably, all the porphyrins show very good sensing performance only towards PA by quenching the emission intensity. Fig. 1 shows the relative fluorescence intensity changes (F_0/F) of freebase as well as tin(IV) porphyrins against various NACs.

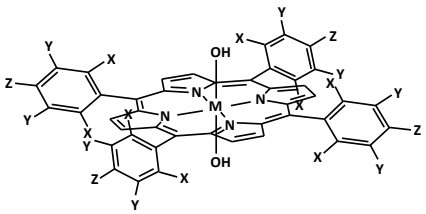

1; M = 2H; X = Y = Z = H; H_2TPP
2; M = 2H; X = Y = H; Z = CH_3; H_2TTP
3; M = 2H; X = Y = H; Z = $COOCH_3$; H_2T(4-CMP)P
4; M = 2H; X = Z = H; Y = OCH_3; H_2T(3,5-OMeP)P
5; M = 2H; X = Y = H; Z = OC_4H_9; H_2T(4-OBuP)P
6; M = Sn; X = Y = Z = H; $Sn^{IV}(OH)_2$TPP
7; M = Sn; X = Y = H; Z = CH_3; $Sn^{IV}(OH)_2$TTP
8; M = Sn; X = Y = H; Z = $COOCH_3$; $Sn^{IV}(OH)_2$T(4-CMP)P
9; M = Sn; X = Z = H; Y = OCH_3; $Sn^{IV}(OH)_2$T(3,5-OMeP)P

Scheme 1 Molecular structure of porphyrins under study.

Bioinorganic Materials Chemistry Laboratory, Department of Chemistry, NIT Calicut, Kozhikode, Kerala-673 601, India. E-mail: arunkumarc@nitc.ac.in; Tel: +914952285307; Fax: +914952287250

† Electronic Supplementary Information (ESI) available: [Additional figures, plots, tables, photophysical data, fluorescence quenching spectra, S–V plots, ORTEP diagrams and X-ray structural data. CCDC: 980779 (**3**·4-NP), 1058018 ($\mathbf{5}^{2+}\cdot PA^{2-}$), 1058017 (**6**·2,4-DNP), 974216 (**6**·PA). See DOI: 10.1039/x0xx00000x

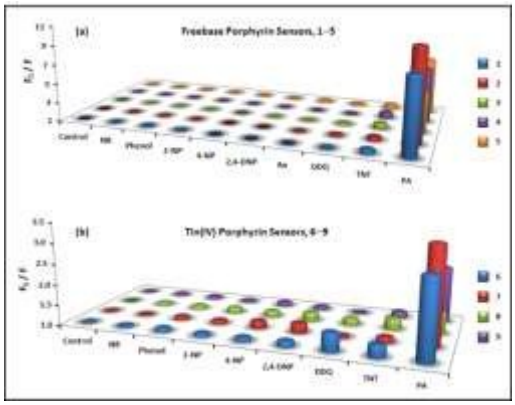

Fig 1 Relative changes in fluorescence intensity (F_0/F) of the fluorophores, (a) **1**–**5** and (b) **6**–**9** against various nitroaromatic compounds.

The turn-off fluorescence response of **2** with different concentration of PA on excitation at 420 nm is shown in Fig. 2a and S2. It is found that the emission intensity of **2** decreases with incremental addition of PA, 90 % quenching was observed for 0.1 μM concentration of PA indicating that there is a strong interaction between **2** and PA. Similar spectral pattern is observed for porphyrins, **1** and **3**–**9** in presence of PA whereas other analytes showed a minor or negligible effect. The selectivity and sensitivity of porphyrins, **1**–**5** towards PA is possibly attributed to the high polarizability of PA and also the presence of strong hydrogen bonding interactions between them. The presence of hydrogen bonding interaction is evident from the crystal structure of the freebase porphyrin–PA complex ($\mathbf{5}^{2+}\cdot 2PA^{-}$). Notably, the quenching efficiency of freebase porphyrins are high compared to tin(IV) derivatives (Fig. 1), which may be due to the decreased electron density at the porphyrin core upon insertion of the metal ion and a similar trend was also observed in zinc(II) porphyrins.[11b] Moreover, the fluorescence quantum yield obtained for freebase porphyrins **2**, **4** and **5** are high ($\phi \approx 0.12$), compared to other porphyrins indicating that they may hold promise for sensing applications.

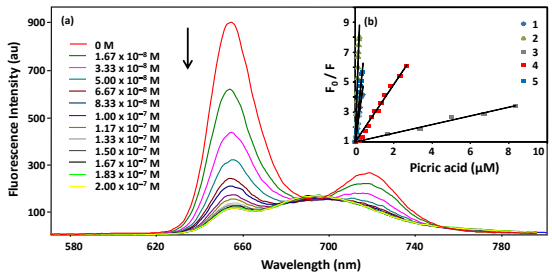

Fig 2 (a) Fluorescence quenching of **2** (1 x 10^{-8} M in $CHCl_3$) upon incremental addition of picric acid (1.67 x 10^{-8} M in $CHCl_3$) (λ_{exc} = 420 nm); (b) Stern–Volmer plots for **1**–**5** against concentration of PA.

The fluorescence quenching of porphyrins against PA at different concentrations was quantitatively evaluated using the Stern-Volmer (S-V) equation.[16] The S-V plots (Fig. 2b) for PA are linear which indicates the existence of static or dynamic quenching process. The increasing order of quenching efficiency of the freebase porphyrins is **2** ≈ **5** > **1** > **4** > **3** and for tin(IV) porphyrins is **7** > **6** ≈ **9** > **8** (Table S2). The given order is in concordant with the electron richness of the porphyrin core. Among the porphyrins, **2** and **5** exhibit a high efficiency for the detection of PA with K_{SV} values of 3.90 x 10^7 M^{-1} and 1.32 x 10^7 M^{-1} respectively. It is the highest quenching constant values among the reported porphyrin-based fluorophores for selective sensing of NACs.[17] and is comparable with the recently reported heavy metal decorated porphyrins (Table S2).[17c] It has been reported that there is no fluorescence quenching for **1** against PA in DMF medium indicating the solvent dependent sensing mechanism.[17c] Interestingly, the purple colour solution of freebase porphyrins, **1**–**5** turned to green upon addition of aliquots of PA, which enables the naked eye detection of picric acid in solution (Fig. 3) whereas tin(IV) porphyrins did not show the colour change. We also performed the control experiments using $CHCl_3$, acetic acid, nitrobenzene, phenol and 2,3-dichloro-5,6-dicyano-1,4-benzoquinone and the freebase porphyrins show negligible fluorescence quenching against them. Whereas the tin(IV) derivative, **6** (Fig. 1) exhibits a lesser magnitude of fluorescence quenching by DDQ and TNT, may be attributed to the hydrogen bonding interactions between the analyte and sensor.

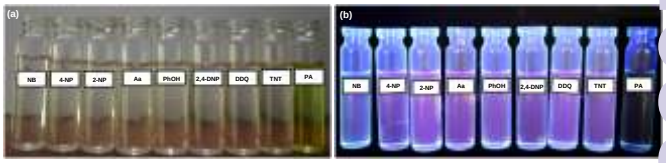

Fig 3 (a) Colorimetric response of **2** (3.3 x 10^{-6} M) with various analytes (3.3 x 10^{-5} M) in chloroform; (i) under normal and (ii) UV-light.

The fluorescence lifetimes of freebase porphyrins and tin(IV) derivatives were measured both in the presence and absence of PA in $CHCl_3$ (Table S3) as portrayed in Fig. S4. In the case of freebase porphyrins, the excited state of the complex ($\mathbf{5}^{2+}\cdot 2PA^{-}$) decays faster than the bare porphyrin suggests that the fluorescence quenching occurs through dynamic mechanism. However, the lifetime is almost invariant at different quencher concentrations for tin(IV) porphyrins, which is possibly due to the axial ligation happened and may correspond to static quenching mechanism occurs through the electron transfer from the electron rich porphyrin to electron deficient PA.

To explore the sensing mechanism involving the protonation of core imino nitrogens, ^{1}H NMR titrations were further carried out for **1** and **6** with PA (0, 1 and 2 equiv.) in $CDCl_3$ (Fig. 4, Fig. S8, S9). Upon titrating **1** with one equiv. of PA, the core protons (-NH) experienced a downfield shift[18] from –2.77 to –1.29 ppm demonstrating the loss of aromaticity leads to nonplanarity. This is due to the protonation occurred in core nitrogen to give porphyrin monoacid observed as a multiplet of β-pyrrole protons specifying the asymmetry nature of the core. Interestingly, the symmetry was regained with the formation of diacid (observed as

singlet for β-pyrrole protons, Fig. 4a) upon addition of one more equivalent of PA, which is subsequently reflected in the increased intensities of -NH peak (Fig. 4a). In the case of **6**, the intensity of *trans*-axial hydroxyl protons signal at −7.42 ppm is disappeared upon increasing the concentration of PA (from 1 to 2 equiv.) indicating the possibility of axial ligation happened in the apex positions (Fig. 4b). These results explicitly corroborate the formation of porphyrin diacid and consistent with the proposed mechanism for the sensing of PA.

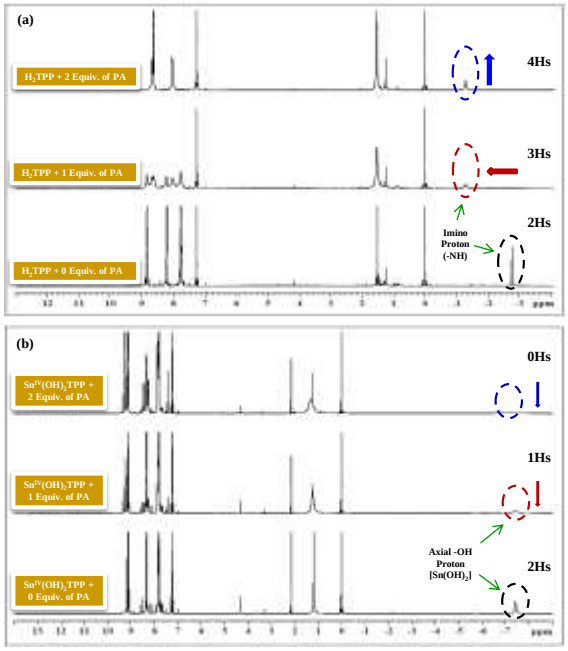

Fig 4 ^{1}H NMR titration of (a) H_2TPP, **1** and (b) $Sn^{IV}(OH)_2$TPP, **6** with picric acid (0, 1 and 2 equiv.) in $CDCl_3$ at 298 K.

The formation of diprotonated species in **1**–**5** in the presence of PA are also visualized from UV-visible spectroscopy. As anticipated, PA selectively interacts with **1–5** showing a considerable red-shift of 26 to 36 nm in the UV-visible spectra (Fig. 5, Fig. S5) and no shifts were observed for other analytes. The UV-visible titration of **2** with the incremental addition of PA is shown in Fig. 5b. Remarkably, a decrement in the absorbance of **2** was observed at 419, 514 nm with the concomitant increment at 448 and 658 nm with an isosbestic point. The Hill plot (Fig. 5b inset) shows a straight line between log[PA] and $\log(A_i-A_0/A_f-A_i)$ with slope value of ~ 2 indicating the stoichiometry ratio between porphyrin to PA is 1:2. And, the higher $\log\beta_2$ value (9.42) demonstrates the efficient interaction between **2** and PA (2 equiv.) which is comparable with the reported diprotonated planar porphyrins.[19] Moreover, the UV-visible spectrum obtained for **2** with PA resembles the optical absorption spectrum of reported diprotonated planar porphyrins[19], $H_4TPP(X)_4^{2+}$ (X = H, CH_3, Ph, Br) in presence of TFA clearly indicates the diacid formation.

The occurrence of protonation in freebase, $\mathbf{5}^{2+}\cdot 2PA^-$ and axial ligation in tin(IV) porphyrins **6**·PA were further unambiguously confirmed by the single crystal X-ray structure data (Table S4, Fig. S6, Fig. S7). To the best of our knowledge, this is the first report for the crystal structure of porphyrin based chemosensors with PA, $\mathbf{5}^{2+}\cdot 2PA^-$ complex and **6**.PA. Single crystals of X-ray quality of **5** with PA was obtained by a slow vapour diffusion of hexane into a chloroform solution of porphyrin that crystallized in orthorhombic crystal system with $P2_12_12_1$ space group. In $\mathbf{5}^{2+}\cdot 2PA^-$ complex, PA exists as picrate ions which are similar to that of reported crystal structure for the tris-imidazolium based sensor.[20] The porphyrin core is found to be *non-planar* (Fig. S6 a-c) and the average mean plane deviation of the β-pyrrole and *meso*-carbon atoms in $\mathbf{5}^{2+}\cdot 2PA^-$ is found to be ± 0.81(2) Å and ± 0.062(2) Å respectively, which is much greater than that of the reported $H_2T(O\text{-}C_4H_9P)PBr_4$[21] bearing antipodal bromine groups (± 0.50(3) Å and ± 0.038 (3) Å). The enhanced non-planarity observed in $\mathbf{5}^{2+}\cdot 2PA^-$ without bulky antipodal bromine groups at the porphyrin periphery indicates the effective interaction between PA and **5** due to their close proximity. Moreover, the intermolecular interactions in $\mathbf{5}^{2+}\cdot 2PA^-$ were found to be mainly of hydrogen bonding between the oxygen atom of the 2,4,6-trinitrophenolate and imino hydrogen of the porphyrin core. It is noteworthy that the hydrogen bonding interactions between porphyrin and PA are very strong owing to their short distances, they found on both faces of the core and in the range of 1.565 – 2.151 Å (N1-H1···O11, 2.073 Å; N3-H3A···O11, 1.951 Å; N2-H2A···O18, 1.565 Å and N4-H4A···O18, 2.151 Å; Figure S6d). Moreover, the weak intermolecular interactions involving hydrogen is 71 % as per the Hirshfeld surface analysis[22] (Fig. S10). But, the co-crystals of **3** with 4-nitrophenol (**3**·4-NP) does not show any non-planarity (Fig. S7a) of the core revealed that the analyte is not good enough to bind with porphyrin, which is also reflected in the fluorimetric titrations.

However, the crystal structure of tin(IV) porphyrins, **6** with the 2,4,6-trinitro phenolate (**6**·PA) and 2,4-dinitro phenolate (**6**·2,4-DNP) moieties were covalently attached to its apex positions through axial ligation (Fig. S7b, S7c). Though the crystal structure of **6**·2,4-DNP was successfully achieved, the fluorimetric titration does not show any turn-off behaviour presumably due to the higher pKa of 2,4-DNP (~ 4) compared to PA (~ 0.4) as well as the lesser affinity of 2,4-DNP towards axial ligation.[23] Hence, the sensing mechanism of these porphyrin chemosensors for the detection of explosive PA is based on the existence of intermolecular proton transfer from PA to freebase porphyrin results in the formation of diprotonated species and axial ligation succeeded in tin(IV) porphyrins (Fig. 6).

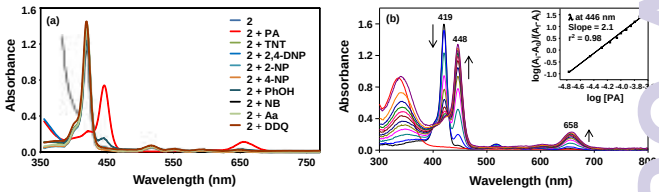

Fig 5 UV-visible spectra of **2** (a) with various analytes and (b) with incremental addition of picric acid.

In summary, freebase and tin(IV) *meso*-tetraarylporphyrins have been explored for its selective detection of powerful explosive PA. The spectroscopic studies revealed that the protonation and axial ligation lead to high fluorescence quenching in freebase and tin(IV) porphyrins respectively which are further evident from single crystal X-ray crystallography. The crystal structure of porphyrin **5** with PA exhibits strong intermolecular hydrogen bonding interactions between the porphyrin diacid and picrate anions. The quenching process is dynamic for freebase and static for tin(IV)-porphyrins. The porphyrins **2** and **5** exhibit highest K_{SV} values (3.90 x 10^7 M^{-1} and 1.32 x 10^7 M^{-1}) among any reported porphyrins, for its selective NACs sensing and thus can serve as efficient chemosensors for the detection of PA.

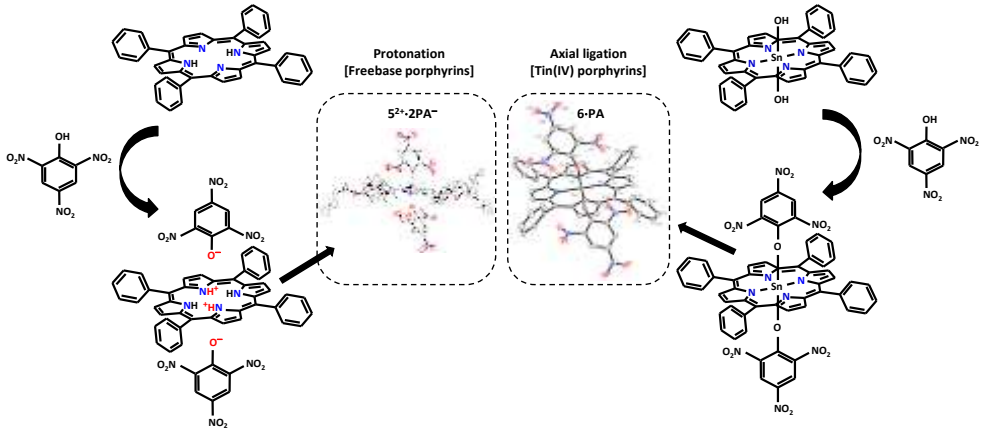

Fig 6 Proposed mechanism of sensing of PA against freebase and tin(IV) porphyrins along with the ORTEP diagrams of 5^{2+}·2PA$^-$ and **6**·PA

Financial support from DST, New Delhi to CA (SB/EMEQ-016/2013) is gratefully acknowledged. We also thank Dr. Shibu M. Eappen, STIC, CUSAT, Kochi and Dr. Babu Varghese, SAIF, IIT Madras, Chennai for the data collection and structure refinement respectively.

Notes and references

1 (a) D. T. McQuade, A. E. Pullen and T. M. Swager, *Chem. Rev.,* 2000, **100**, 2537–2574; (b) M. E. Germain and M. J. Knapp, *Chem. Soc. Rev.,* 2009, **38**, 2543-2555.

2 J. Akhavan, *Chemistry of Explosives*, Royal Society, London, 2nd Edn, 2004.

3 (a) A. P. Demchenko, *Introduction to Fluorescence Sensing,* Springer, 2008; (b) L. B. -Desmonts, D. N. Reinhoudt and M. C. Calama, *Chem. Soc. Rev*., 2007, **36**, 993–1017; (c) K. K. Kartha, S. S. Babu, S. Srinivasan and A. Ajayaghosh, *J. Am. Chem. Soc.,* 2012, **134**, 4834-4841.

4 F. Zhang, L. Luo, Y. Sun, F. Miao, J. Bi, S. Tan, D. Tian and H. Li, *Tetrahedron,* 2013, **69**, 9886-9889.

5 (a) R. Ni, R.-B. Tong, C.-C. Guo, G.-L. Shen and R.-Q. Yu, *Talanta,* 2004, **63**, 251–257; (b) A. Gupta, Y.-A. Kanga, M.-S. Choi and J. S. Park, *Sensors and Actuators B,* 2015, **209**, 225–229.

6 (a) P. B. Pati and S. S. Zade, *Tetrahedron Lett.,* 2014, **55**, 5290-5293; (b) S. Madhu, A. Bandela and M. Ravikanth, *RSC Adv*., 2014, **4**, 7120-7123.

7 (a) W. Wei, R. Lu, S. Tang and X. Liu, *Mater. Chem. A*, 2015, **3**, 4604-4611; (b) Y.-J. Hu, S.-Z. Tan, G.-L. Shen, R.–Q. Yu, *Anal. Chim. Acta*, 2006, **570**, 170–175.

8 S. Chakravarty, B. Gogoi and N. S. Sarma, *J. Luminescence*, 2015, **165**, 6–14.

9 V. Bereau, C. Duhayon and J.-P. Sutter, *Chem. Commun.,* 2014, 12061-12064.

10 (a) X. Jiang, Y. Liu, P. Wu, L. Wang, Q. Wang, G. Zhu, X.-l. Li and J. Wang, *RSC Adv*., 2014, **4**, 47357-47360; (b) Z.-Q. Shi, Z.-J. Guoa and H.-G. Zheng, *Chem. Commun.,* 2015, 8300-8303; (c) S. Sanda, S. Parshamoni, S. Biswas and S. Konar, *Chem. Commun.,* 2015, 6576-6579.

11 (a) F. D'Souza, G. R. Deviprasad and Y. Y. Hsich, *Chem. Commun*., 1997, 533-534; (b) J. Yang, Z. Wang, K. Hu, Y. Li, J. Feng, J. Shi and J. Gu, *ACS Appl. Mater. Interfaces*, 2015, **7**, 11956–11964; (c) M. Ishida, Y. Naruta and F. Tani, *Angew. Chem. Int. Ed.,* 2010, **49**, 91–94; (d) S. Mirra, S. Milione, M. Strianese and C. Pellecchia, *Eur. J. Inorg. Chem.,* 2015, 2272-2276.

12 (a) A. D. Adler, F. R. Longo and J. D. Finarelli, *J. Org. Chem.,* 1967, **32**, 476-476; (b) J. S. Lindsey, I. C. Schreiman, H. C. Hsu, P. C. Kearney and A. M. Marguerettaz, *J. Org. Chem.,* 1987, **52**, 827–836.

13 (a) D. P. Arnold, *J. Chem. Edn*., 1988, **65**, 1111; (b) M. J Crossley, P. Thordarson and R. A.-S. Wu, *J. Chem. Soc. Perkin Trans. 1*., 2001, 2294-2298.

14 M. Meot-Ner and A. D. Adler, *J. Am. Chem. Soc.*, 1975, **975**, 107-111.

15 F. R. Kooriyaden, S. Sujatha and C. Arunkumar, *Polyhedron*, 2015, **97**, 66-74.

16 J. R. Lakowicz, *Principle of Fluorescence Spectroscopy,* Springers, 3rd Edn, 2006.

17 (a) A. Rana and P. K. Panda, *RSC Adv*., 2012, **2**, 12164-12168; (b) S. Tao, G. Li and H. Zhu, *J. Mater. Chem*., 2006, **16**, 4521-4528; (c) P. C. A. Swamy and P. Thilagar, *Chem. Eur. J.,* 2015, **21**, 8874-8882.

18 C. Wang and C. C. Wamser, *J. Org. Chem.,* 2015, **80**, 7351-7359.

19 Y. Fang, P. Bhyrappa, Z. Ou and K. M. Kadish, *Chem. Eur. J.,* 2014, **20**, 524-532.

20 B. Roy, A. K. Bar, B. Gole and P. S. Mukherjee, *J. Org. Chem.,* 2013, **78**, 1306−1310.

21 P. Bhyrappa, C. Arunkumar and B. Varghese, *Acta Cryst.,* 2008, **C64**, o276-o278.

22 M. A. Spackman and D. Jayatilaka, *CrystEngComm.,* 2009, **1** 19-32.

23 Crystal growth obtained for **6** with PA (a week time), with 2,4-DNP (a month time) indicating the relative efficiency of the analytes to attach covalently to the apex positions of the tin(IV) centre.

